Tiled Auxetic Cylinders for Soft Robots

Melanie F. Simons[1,2*], Krishna Manaswi Digumarti[1*], Andrew T. Conn[1,3] and Jonathan Rossiter[1,2]

***Abstract*— Compliant structures allow robots to overcome environmental challenges by deforming and conforming their bodies. In this paper, we investigate auxetic structures as a means of achieving this compliance for soft robots. Taking a tiling based approach, we fabricate 3D printed cylindrical auxetic structures to create tiled auxetic cylinders (TACs). We characterise the relative stiffness of the structures and show that variation in behaviour can be achieved by modifying the geometry within the same tiling family. In addition, we analysed the equivalent Poisson's ratio and found the range between the investigated designs to span from -0.33 to -2. Furthermore, we demonstrate a conceptual application in the design of a soft robot using the auxetic cylinders. We show that these structures can reactively change in shape, thereby reducing the complexity of control, with potential applications in confined spaces such as the human body, or for exploration through unpredictable terrain.**

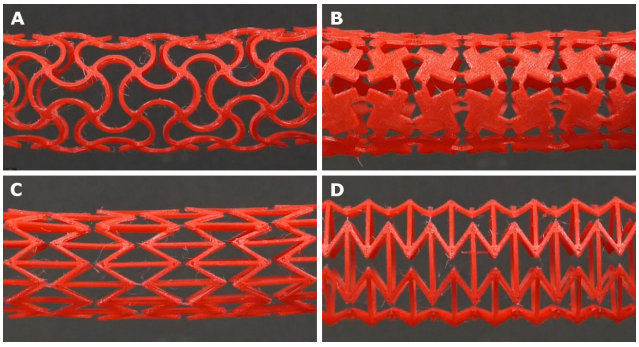

Fig. 1. The four auxetic designs studied are (A) re-entrant sinusoid, (B) modified re-entrant sinusoid, (C) re-entrant hexagon oriented along the axis and (D) re-entrant hexagon oriented perpendicular to the axis.

I. INTRODUCTION

Soft structures give organisms the ability to deform and conform their bodies [1]. This enables them to adapt to challenges in their complex environments. Designs inspired by these structures have been used in the construction of a new generation of robots that are intrinsically compliant, which allows for a high degree of adaptability and agility [2]. Meta-materials have been proposed as a means of designing compliant structures for soft robots [3], which can expand the capability for shape-change within material elastic limits. In this paper, we focus on auxetic structures which are a class of meta-materials. These structures are characterised by a negative Poisson's ratio, i.e. they increase in dimension along a direction perpendicular to that in which they are being stretched.

An advantage of meta-materials is that compliance can be achieved through the use of both soft materials [4] (exhibiting large deformation for the forces that they typically encounter [5]) or rigid materials [6] for structural strength, or a combination of both [7]. This offers greater freedom in the choice of materials when designing a soft robot.

Auxetics have become increasingly popular over the past few years due to their complex and tunable mechanical properties. This is exploited in the design of biomedical devices such as cardiovascular stents [8], deployable structures [9], [10], architecture [11] and energy absorbing foams [12]. Most studies in the literature have focused on two dimensional sheets and three dimensional lattices. A computational estimation of mechanical properties is presented in [13] and an experimental verification of properties in 2D hexagons is presented in [14]. In this paper, we characterise the mechanical properties of auxetic cylinders; planar sheets rolled up into a cylindrical configuration. A cylindrical auxetic has been 3D printed onto a tubular elastomer balloon [15], however we present a simpler process of fabrication in addition to characterising the structures which was absent in that work.

One of the first applications to robot design was presented in [16] where patterns of holes in a 3D printed structure resulted in preferential twisting or bending upon loading. In [3], a 3D auxetic lattice was used in combination with a non-auxetic lattice (positive Poisson's ratio) in a pipe-climbing robot. This study showed a reduction in complexity of the robot's control facilitated by the choice of design, akin to the concept of morphological computation [17]. In a similar vein, a programmed planar sheet was designed in [18] to conform to objects of varied shapes. More recently, sets of handed auxetics [19] have been proposed as a possible alternative to conventional soft robot actuators such as pneumatic networks [20].

Auxetic designs are rarely seen in nature [21] and hence most designs are hand-crafted (inspired for example from ancient motifs [4]) to suit a specific application. In this paper, we take a tiling based approach for the design of auxetics which has been studied in [22]. In particular, we focus on isohedral tiling patterns [23]. These patterns are categorised into classes based on the shape and dimensions of an individual tile. They are further classified into families defined by the pattern of repetition of the minimal repeating unit. A study of mechanical properties (Young's modulus, Poisson's ratio and bending stiffness) of sheet materials designed using isohedral tilings is presented in [24]. Though the

[1]Bristol Robotics Laboratory, University of Bristol, BS16 1QY, UK.
[2]Dept. of Engineering Mathematics, University of Bristol, BS8 1UB, UK
[3]Dept. of Mechanical Engineering, University of Bristol, BS8 1TR, UK
*MFS and KMD contributed equally (and are joint first authors) melanie.simons@bristol.ac.uk, km.digumarti@bristol.ac.uk

study provides indication of the auxetic property of certain patterns, this behaviour was not explicitly investigated. An advantage of the tile based approach is that it is conducive to parameterisation. This implies that the structures can be tuned to achieve desirable mechanical properties. Indeed, we demonstrate this change in behaviour in our work.

This paper records the characterisation of four different auxetic structures that have been constructed into a cylindrical shape. We call these tiled auxetic cylinders (TACs). The elongation force required to stretch the auxetic structure in length and the change in diameter are analysed. Comparisons are made between the various auxetic designs in terms of changes in these properties. Furthermore, an application within robotics of these TACs is illustrated.

II. DESIGN

A. Fabrication

The auxetic structures presented in this work were 3D printed in a single plane on a desktop 3D printer (Wanhao Duplicator i3) with thermoplastic polyurethane (TPU, rigid.ink, Youngs modulus = 15.5MPa [24], Poisson's ratio = 0.48 [25], Shore A Hardness: 94A). The thickness of each sheet was 1mm. They were then rolled up to form a cylindrical structure that bonded together place with adhesive (Ethyl 2-cyanoacrylate, Loctite superglue). The flexible nature of the material facilitated the construction of a 3D structure from a 2D sheet. Loops were printed on the structure so that the free ends of the cylinder could be suitably clamped in the experiments that characterise their mechanical properties.

B. Auxetic Design

Four different auxetic designs were studied, which were all re-entrant structures. The first two designs (A and B in fig. 1) are re-entrant sinusoids [26] and the second two (C and D in fig. 1) are re-entrant hexagons [27]. The difference between the two hexagons is the orientation of the pattern with respect to the axis of the cylinder. The designs are referred to as being oriented along the axis (C in fig. 1) and perpendicular to the axis (D in fig. 1) based on the angle that that the parallel rods make with the longitudinal axis of the cylinder.

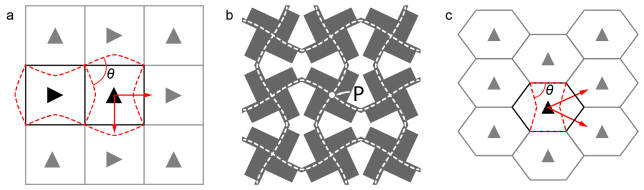

Fig. 2. (a) Isohedral tiling pattern with square tiles. Triangles indicate orientation of tiles. Arrows indicate tiling directions. Dotted line shows a re-entrant sinusiod on the minimal repeating unit. (b) Re-entrant sinusoid (dotted line) overlaid on the modified re-entrant sinusoid (grey) showing that both the structures belong to the same isohedral tiling family. The point P that is common to four neighbouring tiles is the point of rotation. (c) Isohedral tiling pattern with hexagonal tiles. In this case, all the tiles have the same orientation. The re-entrant hexagon is shown with a dotted line. θ denotes the re-entrant angle.

The re-entrant sinusoid designs belong to the same family of isohedral tiling [28], which can be described as a pattern of square tiles (fig. 2a). They are effectively the same design, the difference being that the latter, referred to here as the modified re-entrant sinusoid, has enlarged rotation points that makes it stiffer than the simple re-entrant sinusoid (point P in fig. 2b). The smallest repeating unit in the pattern is a pair of adjacent tiles oriented perpendicular to each other (fig. 2a).

The hexagonal designs belong to belong to a family with hexagonal tiles which are arranged next to each other in the same orientation (fig. 2c) rather than perpendicular to its neighbouring tile as seen in the sinusoidal designs. The re-entrant hexagon structure was orientated in two different ways to create the cylindrical structure: along the axis and perpendicular to the axis.

These four designs have been selected to illustrate the effect of change in geometry and orientation of patterns on mechanical properties when they belong to the same family of tilings. Several other patterns exist such as arrowheads [12], stars [13] and chiral geometries [10],[12],[13]. Their analysis, including different orientations, will be considered in future studies.

III. EXPERIMENTAL METHOD

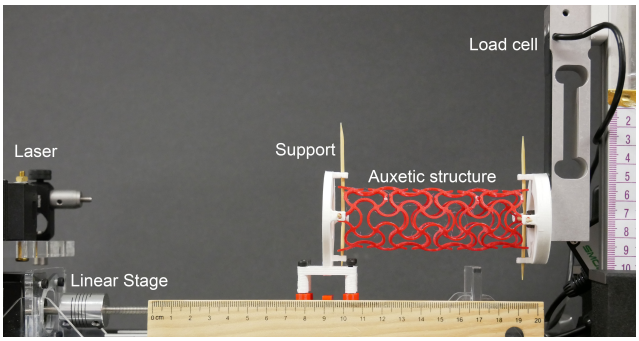

Fig. 3. The experimental setup used to determine the relationship between elongation force and elongation in length of a cylindrical auxetic structure.

To measure the relationship between elongation force and length, the cylindrical structures were held in a linear stage with the axis parallel to the horizontal (fig. 3). One end of the cylinder was fixed to a load cell (Model no. 1022, Tedea-Huntleigh, max. load 5kg) while the other end was connected to the moving carriage which moved at a constant rate of 0.45mm/s imposing an elongation in length. Two wooden supports were inserted into the diametrically opposite loops at each free end of the cylinder, oriented perpendicular to one another and to the axis of the cylinder resulting in four points of contact at either end. The rotation of the structure was thus constrained, while allowing it to freely increase in diameter upon elongation in length. The position of the carriage was measured using a laser displacement sensor (LK-G512 and LKGD500, Keyence). Both elongation force and displacement readings were recorded using a data acquisition system (USB-6001, National Instruments) at a frequency of 1000Hz. The experiment was repeated 10 times for each design.

Each experiment was recorded on video (DMC-G80, Panasonic) at a constant rate of 60fps. Individual frames from the video were then analysed in MATLAB using a computer vision program to extract the diameter of the complete structure (defined as the maximum span of a 2cm wide region in the middle of the structure) as it changed with its entire length.

IV. RESULTS

A. Deformation of the Structure

A close up of the structure's deformation upon elongation in length for the four designs is shown in fig. 4. In the case of the re-entrant sinusoids (A and B in fig. 4), the curved edges straightened out during elongation. This can be seen as a rotation of the square patches in the case of the second design. In the third design, a three-dimensional buckling of the structure was observed. In the final design, curving of elements forming the re-entrant portion of the structure was seen.

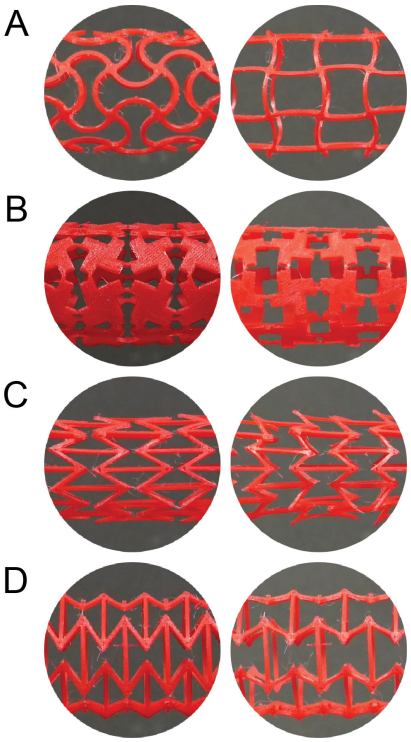

Fig. 4. Configuration of the structure at rest (left) and after elongation (right) for the four designs considered: (A) re-entrant sinusoid, (B) modified re-entrant sinusoid, (C) re-entrant hexagon oriented along the axis and (D) re-entrant hexagon oriented perpendicular to the axis.

B. Force-Elongation Relationship

The relation between elongation force and elongation in length is shown in fig. 5. Both the re-entrant sinusoid (A) and modified re-entrant sinusoid (B) exhibit stiffening, with the latter more stiffening at a smaller elongation. This is expected as the points of rotation (P in fig. 2b) were designed to be stiffer in B. In the case of the re-entrant hexagons, two distinct behaviours are observed based on the orientation of the pattern in the cylinder. In the case of the pattern oriented along the axis of the cylinder (C), a stiffening behaviour is observed initially, followed by a softening of the structure. This can be attributed to the out of plane deformation that was observed in the structure (C in fig. 4 (right)). The relation between elongation force and elongation in length is approximately linear in the final case (D) where the structure was oriented perpendicular to the axis. A gentle stiffening was observed at larger elongations due to deformation of the re-entrant beam elements (D in fig. 4 (right)). The low standard deviation in all the cases demonstrates that the behaviour is repeatable.

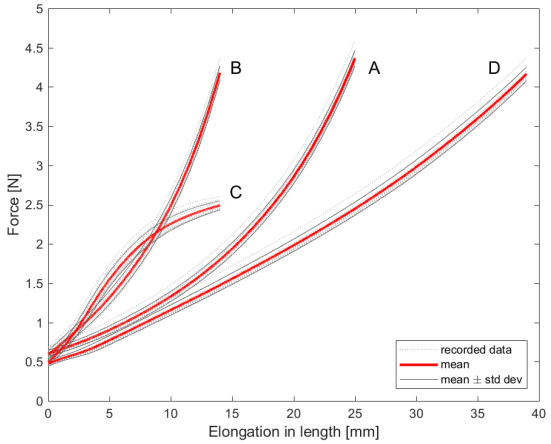

Fig. 5. Relation between elongation force and elongation for the four auxetic designs considered: (A) re-entrant sinusoid, (B) modified re-entrant sinusoid, (C) re-entrant hexagon oriented along the axis and (D) re-entrant hexagon oriented perpendicular to the axis. The dotted lines indicate recorded data, the solid red line indicate the mean of 10 trials and the thin solid lines indicate one standard deviation away from the mean.

C. Diameter-Length Relationship

The relation between normalised change in diameter and normalised change in length for the four auxetic structures is shown in fig. 6. In all the cases, the relation was found to be linear. The negative of the slope of the curve can be interpreted as an equivalent Poisson's ratio for the structure since the Poisson's ratio defined for non-auxetic structures considers a decrease in dimension perpendicular to that of extension rather than an increase as seen here. These values are reported in table I. They are comparable to those presented in [13] for flat sheets; -0.81 for the re-entrant sinusoid and -0.34 for the re-entrant hexagon when the orientation is perpendicular to the axis. Elastomers are the predominant soft robotic material and are widely considered to have a Poisson's ratio approximately equal to 0.5.

V. DISCUSSION

The behaviour of the four different TAC structures studied show similarities as well as differences. The relation between elongation force and displacement (fig. 5) is an indication

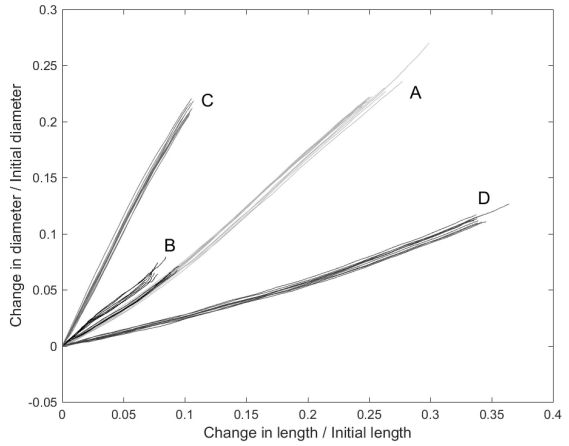

Fig. 6. Relation between normalised change in diameter and normalised change in length for the four auxetic designs considered: (A) re-entrant sinusoid, (B) modified re-entrant sinusoid, (C) re-entrant hexagon oriented along the axis and (D) re-entrant hexagon oriented perpendicular to the axis.

Design	Equivalent Poisson's ratio
(A) Re-entrant sinusoid	-0.90 $\pm$ 0.01
(B) Modified re-entrant sinusoid	-0.76 $\pm$ 0.08
(C) Re-entrant hexagon $\parallel$ axis	-2.09 $\pm$ 0.05
(D) Re-entrant hexagon $\perp$ axis	-0.33 $\pm$ 0.01

TABLE I

EQUIVALENT POISSON'S RATIO FOR THE FOUR AUXETIC STRUCTURES.

of the effective Young's modulus. Here we present the elongation force instead of the stress because it is not trivial to determine the area of cross section, which changes as the structure elongates and the material is stretched. The relation between the normalised change in diameter and normalised change in length (fig. 6) is an indication of the Poisson's ratio.

The two re-entrant sinusoid structures (A and B in fig. 1) showed the most similarities. In the case of the elongation force measurement with elongation of the structure (fig. 5), the shape of the curves are the same, but with a steeper curve seen for the modified re-entrant sinusoid (B) compared with the original re-entrant sinusoid (A). This is due to the enlarged rotation points (point P in fig. 2) making the structure stiffer overall. It may be deduced that structures with stiffness in the range between these two curves can be obtained by changing the amount of material at the points of rotation. The equivalent Poisson's ratios (table I) for both are similar at a value close to -1. In fig. 6 the curves follow the same trajectory which reinforces this similarity, where the modified re-entrant sinusoid shows a smaller change in length and diameter, again due to its increased stiffness.

The larger proportion of solid surface area in the modified re-entrant sinusiod (B) relative to (A), also highlights the potential for design control over relative areal porosity change during expansion. For example, a 10% extension in length generates a relative surface porosity increase of 12% in B and 5% in A.

The two re-entrant hexagonal structures (C and D in fig. 1), though they are the exact same structure, show very different properties due to their different alignment relative to the axis of the cylinder. The re-entrant hexagon orientated perpendicular to the axis (D) is most comparable to the re-entrant sinusoid designs, where the relation between the elongation force and elongation (fig. 5) is slightly more linear. The re-entrant hexagon orientated along the axis (C), however, shows a rather different relation between elongation force and elongation. Initially it shows stiffening similar to the modified re-entrant sinusoid (B). The structure then softens owing to the out of plane deformation of the parallel rods (C in fig. 4, right). This could be attributed to high stress concentration in the angular joints and the curving out of the structure to attain a minimal energy state. This is an interesting behaviour and can potentially be exploited for locomotion [29]. This is not observed in the other structures due to the nature of the design which provides a continuous beam from one end to the other, thus preventing out of plane deformation. A detailed investigation will be addressed in a future work. The equivalent Poisson's ratios are also very different. The former (D) demonstrates a large equivalent Poisson's ratio at -2, approximately twice that of the re-entrant sinusoid structures. When the same structure is orientated at 90° (C), the equivalent Poisson's ratio is less than a quarter at -0.33.

Interesting to note are the behavioural differences between the two tiling families. Elongation in structures A and B is due to the points of rotation (point P in fig. 2) where the re-entrant angle (θ in fig. 2) remains constant. Elongation of structures C and D however is due to a change in the re-entrant angle. This relationship between re-entrant angle and elongation of the structure will be investigated in future work.

Throughout analysis of the experimental results, it was assumed that the behavioural properties were as a result of the hinges in the structural design alone. Future work will look at the combined behaviours of structural expansion and material extension.

The behaviour of the TACs can be compared to that of other classes of soft robotic structures. Here we compare the conceptual relation between diameter and length. The structures chosen for comparison are McKibben actuators, ideal balloon, standard bellows, hyperelastic bellows (HEB, [30]) and solid elastomers. This comparison is shown in fig. 7. The behaviour of the auxetic structure is linear and is similar to that of an ideal balloon. The slope of the curve can be tuned and various structures display varied magnitudes of steepness (fig. 6). Unlike in the case of the HEB, there is no region of decoupling between length and diameter. Both these dimensions increase or decrease simultaneously.

VI. SOFT ROBOTIC APPLICATION

To demonstrate a conceptual application of TACs to the design of soft robots, we considered the case of an auxetic cylindrical unit moving through a pipe. The design in this case was along the lines of the modified re-entrant sinusoid.

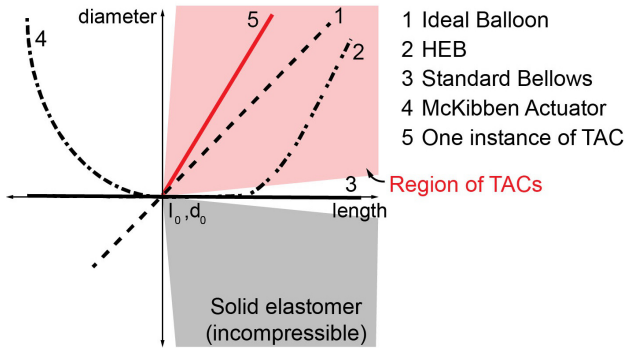

Fig. 7. Comparison of TACs with various classes of structures showing the conceptual relation between diameter and length during actuation. All structures are assumed to have an initial length of l_o and diameter d_o. Adapted from [30].

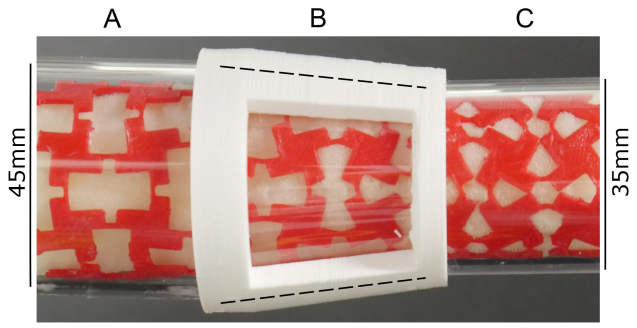

Fig. 8. Demonstration of the change in shape of an auxetic cylinder as it moves through a constricted space. The structure is in its fully expanded configuration in the wider region (A), partially contracted in the constriction (B) and fully contacted in the smaller tubular region (C).

However, the design is slightly different from that presented in sec. II-B in terms of the configuration at rest. The design presented previously was 3D printed in a contracted configuration (fig. 4B, left) whereas the design considered here was printed in an expanded configuration similar to that in the elongated state shown in fig. 4B (right). This implies that the structure is expanded in its natural resting configuration and is an example of how the zero energy state can be controlled. In this configuration, the elastic biasing force will drive it towards expansion. The initial diameter of this structure was 45mm and it could contract to 35mm.

The structure was made to move through an acrylic pipe, the internal diameter of which was 45mm, sufficiently large to accommodate it in its rest configuration. Motion was achieved through an external longitudinal force. A constriction to motion was provided in the form of a decrease in diameter of the pipe. This was achieved using a 3D printed conical part. At the other end of the constriction, a second pipe of smaller diameter (35mm) was attached that allowed the structure to pass through only in its contracted configuration but not in its expanded configuration.

As the structure moves through the constriction, reactive forces from the walls of the constriction acting on the structure cause a contraction in length which result in a reduction in diameter, thus allowing the structure to pass through. The change in configuration of the auxetic can be clearly seen in fig. 8. In the larger diameter tube, the structure is in a fully expanded configuration (fig. 8A). This is followed by a partially contracted configuration in the constriction (fig. 8B) and a fully contracted configuration in the smaller pipe (fig. 8C).

In this demonstration, the change in shape is not actively controlled but is caused by the structure reacting to a change in the environment in which it is operating. In this sense, the design of the structure is contributing to its control. In other scenarios, where active control of shape is desired, the auxetic structure can still provide this ability. This is an advantage over soft robot designs that purely depend on soft material to passively conform to objects that they interact with.

The internal foam prevents buckling of the structure on compression, however we believe that it does not contribute to the auxetic behaviour. Further study will look at characterising these TACs printed in various states of expansion. This demonstration illustrates the potential use of these TACs for pipe inspection or cleaning, where the structure still allows flow through the pipe.

VII. CONCLUSION

In this paper, we have investigated TACs; a tiling pattern based approach to the design of cylindrical auxetic structures. We focused on two particular designs, the re-entrant sinusoid and the re-entrant hexagon. We characterised the structures in terms of the elongation force and diameter as they change with elongation. Our analysis showed that a minor modification of the design within the same family of tiling can result in a significant difference in behaviour. In addition, we showed the emergence of variation in behaviour by simply altering the orientation of the pattern within the structure.

The tiling based approach is amenable to parameterisation. This allows for tuning the design to achieve a desired mechanical response. Following this work, there is scope for more study. Transition between multiple designs within the same structure and the impact of this on mechanical properties will also be studied in future work. Regions with varying stiffness could potentially be created at specific locations on the structure leading to interesting and emergent macroscopic behaviours. The rest configuration of the 3D printed structure affects its stiffness. The preference for a more contracted or more expanded configuration could be exploited in the design of a robot. This is another topic for investigation.

The conceptual demonstration of a soft robot application showed the reactive change in shape of the auxetic structure when moving through a constriction. This property has potential applications in robots designed to move through confined spaces such as in the human body and subterranean exploration where the robot can reconfigure itself relative to its surroundings with minimal complexity of control.

ACKNOWLEDGMENT

This work was supported by the EPSRC Centre for Doctoral Training in Future Autonomous and Robotic Systems (FARSCOPE, grant EP/L015293/1) at the Bristol Robotics Laboratory where KMD is a PhD student. MFS was supported by EPSRC DTP grant. AC was supported by EPSRC grant EP/P025846/1. JR was supported by EPSRC grants EP/M020460/1 and EP/M026388/1 and was also funded by the Royal Academy of Engineering as a Chair in Emerging Technologies.

REFERENCES

[1] S. Kim, C. Laschi, and B. Trimmer, "Soft robotics: a bioinspired evolution in robotics," *Trends in biotechnology*, vol. 31, no. 5, pp. 287–294, 2013.

[2] D. Rus and M. T. Tolley, "Design, fabrication and control of soft robots," *Nature*, vol. 521, no. 7553, p. 467, 2015.

[3] A. G. Mark, S. Palagi, T. Qiu, and P. Fischer, "Auxetic metamaterial simplifies soft robot design," in *Robotics and Automation (ICRA), 2016 IEEE International Conference on*, pp. 4951–4956, Ieee, 2016.

[4] A. Rafsanjani and D. Pasini, "Bistable auxetic mechanical metamaterials inspired by ancient geometric motifs," *Extreme Mechanics Letters*, vol. 9, pp. 291 – 296, 2016.

[5] B. Trimmer and H. Lin, "Bone-free: Soft mechanics for adaptive locomotion," 2014.

[6] R. Naboni and L. Mirante, "Metamaterial computation and fabrication of auxetic patterns for architecture," *SIGRADI Conference Paper: Digital Manufacturing & Rapid Prototyping*, pp. 129–136, 2015.

[7] K. Wang, Y.-H. Chang, Y. Chen, C. Zhang, and B. Wang, "Designable dual-material auxetic metamaterials using three-dimensional printing," *Materials & Design*, vol. 67, pp. 159 – 164, 2015.

[8] T. Wei Tan, G. R. Douglas, T. Bond, and A. S. Phani, "Compliance and longitudinal strain of cardiovascular stents: Influence of cell geometry," *Journal of Medical Devices*, vol. 5, pp. 041002–1 – 041002–6, 12 2011.

[9] A. T. Conn and J. Rossiter, "Smart radially folding structures," *IEEE/ASME Transactions on Mechatronics*, vol. 17, pp. 968–975, Oct 2012.

[10] J. Rossiter, K. Takashima, F. Scarpa, P. Walters, and T. Mukai, "Shape memory polymer hexachiral auxetic structures with tunable stiffness," *Smart Materials and Structures*, vol. 23, no. 4, p. 045007, 2014.

[11] G. Fallacara, M. Barberio, and M. Colella, "Learning by designing: Investigating new didactic methods to learn architectural design," *Turkish Online Journal of Educational Technology*, pp. 455–465, 2017.

[12] M. Sanami, N. Ravirala, K. Alderson, and A. Alderson, "Auxetic materials for sports applications," *Procedia Engineering*, vol. 72, pp. 453 – 458, 2014. The Engineering of Sport 10.

[13] J. C. Á. Elipe and A. D. Lantada, "Comparative study of auxetic geometries by means of computer-aided design and engineering," *Smart Materials and Structures*, vol. 21, no. 10, p. 105004, 2012.

[14] F. Scarpa, P. Panayiotou, and G. Tomlinson, "Numerical and experimental uniaxial loading on in-plane auxetic honeycombs," *The Journal of Strain Analysis for Engineering Design*, vol. 35, no. 5, pp. 383–388, 2000.

[15] F. B. Coulter and A. Ianakiev, "4d printing inflatable silicone structures," *3D Printing and Additive Manufacturing*, vol. 2, no. 3, pp. 140–144, 2015.

[16] A. Lazarus and P. M. Reis, "Soft actuation of structured cylinders through auxetic behavior," *Advanced Engineering Materials*, vol. 17, no. 6, pp. 815–820, 2015.

[17] R. Pfeifer and J. Bongard, *How the body shapes the way we think: a new view of intelligence*. MIT press, 2006.

[18] M. J. Mirzaali, S. Janbaz, M. Strano, L. Vergani, and A. A. Zadpoor, "Shape-matching soft mechanical metamaterials," *Scientific Reports*, vol. 8, pp. 965:1 – 965:7, 2018.

[19] J. I. Lipton, R. MacCurdy, Z. Manchester, L. Chin, D. Cellucci, and D. Rus, "Handedness in shearing auxetics creates rigid and compliant structures," *Science*, vol. 360, no. 6389, pp. 632–635, 2018.

[20] B. Mosadegh, P. Polygerinos, C. Keplinger, S. Wennstedt, R. F. Shepherd, U. Gupta, J. Shim, K. Bertoldi, C. J. Walsh, and G. M. Whitesides, "Pneumatic networks for soft robotics that actuate rapidly," *Advanced functional materials*, vol. 24, no. 15, pp. 2163–2170, 2014.

[21] V. Carneiro, J. Meireles, and H. Puga, "Auxetic materials a review," *Materials Science-Poland*, vol. 31, pp. 561–571, 10 2013.

[22] C. Borcea and I. Streinu, "Geometric auxetics," *Proc. R. Soc. A*, vol. 471, no. 2184, p. 20150033, 2015.

[23] C. S. Kaplan and D. H. Salesin, "Escherization," in *Proceedings of the 27th Annual Conference on Computer Graphics and Interactive Techniques*, SIGGRAPH '00, (New York, NY, USA), pp. 499–510, ACM Press/Addison-Wesley Publishing Co., 2000.

[24] C. Schumacher, S. Marschner, M. Cross, and B. Thomaszewski, "Mechanical characterization of structured sheet materials," *ACM Trans. Graph.*, vol. 37, pp. 148:1–148:15, July 2018.

[25] H. Qi and M. Boyce, "Stressstrain behavior of thermoplastic polyurethanes," *Mechanics of Materials*, vol. 37, no. 8, pp. 817 – 839, 2005.

[26] Y. Liu and H. Hu, "A review on auxetic structures and polymeric materials," *Scientific Research and Essays*, vol. 5, no. 10, pp. 1052–1063, 2010.

[27] H. A. Kolken and A. A. Zadpoor, "Auxetic mechanical metamaterials," *RSC Adv.*, vol. 7, pp. 5111–5129, 2017.

[28] C. S. Kaplan, *Introductory Tiling Theory for Computer Graphics*. Morgan and Claypool Publishers, 2009.

[29] A. Rafsanjani, Y. Zhang, B. Liu, S. M. Rubinstein, and K. Bertoldi, "Kirigami skins make a simple soft actuator crawl," *Science Robotics*, vol. 3, no. 15, p. eaar7555, 2018.

[30] K. M. Digumarti, A. T. Conn, and J. Rossiter, "Euglenoid-inspired giant shape change for highly deformable soft robots," *IEEE Robotics and Automation Letters*, vol. 2, no. 4, pp. 2302–2307, 2017.